A realistic dynamic blower energy consumption model for wastewater applications

Y. Amerlinck, W. De Keyser, G. Urchegui and I. Nopens

ABSTRACT

At wastewater treatment plants (WWTPs) aeration is the largest energy consumer. This high energy consumption requires an accurate assessment in view of plant optimization. Despite the ever increasing detail in process models, models for energy production still lack detail to enable a global optimization of WWTPs. A new dynamic model for a more accurate prediction of aeration energy costs in activated sludge systems, equipped with submerged air distributing diffusers (producing coarse or fine bubbles) connected via piping to blowers, has been developed and demonstrated. This paper addresses the model structure, its calibration and application to the WWTP of Mekolalde (Spain). The new model proved to give an accurate prediction of the real energy consumption by the blowers and captures the trends better than the constant average power consumption models currently being used. This enhanced prediction of energy peak demand, which dominates the price setting of energy, illustrates that the dynamic model is preferably used in multi-criteria optimization exercises for minimizing the energy consumption.

Key words | aeration, centrifugal blowers, energy, optimisation, positive displacement blowers, submerged diffusers

Y. Amerlinck (corresponding author)
W. De Keyser
I. Nopens
BIOMATH, Department of Mathematical Modelling, Statistics and Bioinformatics,
Ghent University,
Coupure Links 653,
Gent 9000,
Belgium
E-mail: *youri.amerlinck@ugent.be*

G. Urchegui
MONDRAGON SISTEMAS, S. COOP. (MSI),
AmaKandida, 21 DENAC,
Andoain 20140,
Gipuzkoa,
Spain

GLOSSARY

A,B,C	Parameters of the generic blower curve based on N (–)
A_{PL},B_{PL},C_{PL}	Parameters of the power law (–)
A_{QL},B_{QL},C_{QL}	Parameters of the quadratic law (–)
BC	Blower curve
BC_{VFD}	Blower curve when controlled by a variable-frequency drive
d	Air line inside diameter (mm)
f_{IGV}	Guide vane opening fraction (–)
f_{Diff}	Linear pressure loss factor (m H_2O/(Nm^3/(h·m^2)))
$f_{fouling}$	Fouling factor (–)
$f_{fouling,max}$	Maximum fouling factor (–)
FP	Fraction of the power consumption at full load (–)
FPL	Friction power loss at actual operating conditions (kW)
g	Gravitational acceleration (m/s^2)
H_0	Cut-off head (m H_2O)
H_w	Height of water above the diffusers (m)
k	Experimental scaling factor (–)
K_v	Valve-specific flow factor (Nm^3/h)
L	Air line length (m)
L_{equiv}	Equivalent pipe length (m)
$L_{fittings}$	Equivalent pipe length for fittings (m)
L_{pipe}	Real pipe length (m)
N	Relative blower speed (–)
n	Dimensionless constant for air (0.285) (–)
$N_{desired}$	Desired relative blower speed (–)
OP	Operating point
$OP_{throttling}$	Operating point when controlled with outlet throttling
OP_{VFD}	Operating point when controlled by a variable-frequency drive
p_{blower}	Blower outlet pressure (kPa)
p_{in}	Inlet pressure (kPa)
p_m	Mean system pressure (kPa)
p_{out}	Pressure at the blower outlet (kPa)
$p_{out,IGV}$	Pressure at the blower outlet in the case of inlet guide vane control (kPa)

doi: 10.2166/wst.2016.360

p_{std}	Atmospheric pressure at sea level (kPa)
P	Power draw (kW)
P_{actual}	Actual power draw (kW)
PV_a	Saturated vapour pressure of water (kPa)
Q_1, Δp_1	Flow rate – pressure combination on the blower curve (Nm³/h, kPa)
Q_2, Δp_2	Flow rate – pressure combination on the blower curve (Nm³/h, kPa)
Q_3, Δp_3	Flow rate – pressure combination on the blower curve (Nm³/h, kPa)
Q_{Air}	Airflow rate (Nm³/h)
$Q_{Air,actual}$	Actual airflow rate (Nm³/h)
$Q_{Air,desired}$	Desired airflow rate (Nm³/h)
$Q_{Air,in}$	Incoming air flow rate (Nm³/h)
$Q_{Air,in,N}$	Normalized volumetric air flow rate (Nm³/h)
Q_{BEP}	Airflow rate at which the best efficiency is reached (Nm³/h)
Q_{design}	Design airflow rate (Nm³/h)
Q_{max}	Maximum airflow rate (Nm³/h)
Q_0	Blower's theoretical airflow rate at full speed and $p_{out} = p_{in}$ (Nm³/s)
R	Universal gas constant (J/(K.mol))
RH	Relative humidity (–)
SC	System curve
$SC_{throttling}$	System curve when controlled with outlet throttling
t	Time (d)
$t_{last\ cleaning}$	Last cleaning time (d)
T_{in}	Air temperature at the blower inlet (K)
Z	Altitude above sea level (m)
α, β	Experimental scaling factors (–)
η_m	Mechanical efficiency (–)
η_{max}	Maximum efficiency (–)
η_{min}	Minimum efficiency (–)
η_e	Electrical efficiency (–)
η_p	Pneumatic efficiency (–)
η_v	Volumetric efficiency (–)
η_{VFD}	Variable frequency drive efficiency (–)
η_t	'Wire-to-air' efficiency or total efficiency (–)
$\eta_{\text{throttling}}$	Efficiency for outlet throttling control (–)
ρ_{air}	Relative specific gravity of air (kg/m^3)
ρ_w	Density of the water (kg/m^3)
Δ_η	Difference between the maximum and minimum efficiency (–)
Δp_{design}	Design pressure difference (kPa)
Δp_{DWP}	Diffuser dynamic wet pressure (kPa)
Δp_{line}	Pressure losses in the air line (kPa)
Δp_{max}	Maximum pressure (kPa)
Δp_{system}	Total pressure loss in the system (kPa)
Δp_w	Water head above the diffuser (kPa)
$\Delta t_{cleaning}$	Periods in between consecutive cleaning (kPa)

INTRODUCTION

One of the main challenges for the optimization of wastewater treatment plants (WWTPs), today, is the proper evaluation of all important performance indicators such as effluent quality (including priority pollutants), energy consumption and greenhouse gas emissions. At WWTPs aeration is the largest energy consumer (Tchobanoglous *et al.* 2004; Devisscher *et al.* 2006; Ast *et al.* 2008; Fenu *et al.* 2010; Zahreddine *et al.* 2010) and as such aeration energy consumption and related costs are an essential factor to be considered in the optimization of WWTPs.

Key factors that influence WWTP aeration cost are the type of aeration blower employed, the aeration system configuration (e.g. diffuser types, water head and piping characteristics) and the control strategy implemented on the aeration system. In addition it is important to consider the application of different energy pricing structures (e.g. time-of-use rates) and charges (e.g. energy usage, peak power demand charges) in the different billing terms (Aymerich *et al.* 2015). In order to appropriately consider the different energy pricing structures one needs a time varying or dynamic prediction of the energy consumption.

The blowers employed in fine bubble diffuser aeration systems are compressors operating at low relative pressures and can be classified into two broader classes, i.e. centrifugal and positive displacement (PD) types (Henze 2008). To date, three main control strategies are implemented to enable 'turn-up' or 'turn-down' capacity of these aeration blowers, namely variable inlet guide vane (IGV) control, outlet throttling (OT) control and variable frequency drive (VFD) control.

Despite the increasing level of detail in wastewater treatment process models, oversimplified energy consumption models (i.e. constant 'average' power consumption), without any mechanistic knowledge, are still being used in design and optimization exercises (Copp 2002; Rosso & Stenstrom 2005; Gernaey *et al.* 2006; Martín de la Vega *et al.* 2013; Wambecq *et al.* 2013). Only a few publications mention the idea of including more rigour in modelling the aeration

supply side but they fail to give a clear description of the details and implementation (Alex *et al.* 2002; Beltrán *et al.* 2011; Arnell & Jeppsson 2015). As these wastewater treatment process models have the interesting potential to be used in multi-criteria optimization exercises (e.g. optimizing effluent quality, greenhouse gas emissions and operational costs simultaneously (Flores-Alsina *et al.* 2014), they may lead to poor predictions and their use in optimization could lead to sub-optimal operation. There is a clear hiatus in knowledge specifically with regard to rigorous mechanistic models for energy or cost optimisation of these systems. As described above, such models have not yet been reported.

This paper aims at developing an original and novel dynamic model for more accurate prediction of aeration energy costs in activated sludge systems, equipped with submerged air distributing diffusers (producing coarse or fine bubbles) connected via piping to blowers. This is needed to overcome the imbalance in the coupled sub-models (Amaral *et al.* 2016). The objective of the proposed model is to allow for dynamically and accurately simulating the power consumed by an aeration system as a function of (a) the physical characteristics of the aeration system (i.e. blowers, piping, diffusers), (b) the water height in the aerated tanks and (c) the volumetric air flow rate imposed by a control system. The remainder of the paper will illustrate the dynamic model, its calibration and application to the WWTP of Mekolalde (Spain). Finally, a comparison is made with the currently frequently used average power consumption models, and the preferable use of the newly proposed model in optimisation efforts for energy cost minimisation is explained.

MATERIALS AND METHODS

Centrifugal and PD blowers

Similar to pumps, aeration blowers are classified into two main categories: (i) centrifugal blowers and (ii) PD blowers. Centrifugal blowers, sometimes referred to as dynamic type blowers, have the air intake along the axis of rotation at the impeller centre and continuously discharge air radially. This rotational action increases the kinetic energy within the air stream, thereby increasing the pressure over the system (Henze 2008).

PD blowers utilise a different approach compared to that of centrifugal blowers by virtually moving 'batches' of air from the blower inlet to the oulet (Henze 2008). The result is that PD blowers have the capacity to operate against higher ouput pressures than centrifugal blowers for the same air flow rates (Henze 2008). However, the efficiencies of PD blowers are lower than those of centrifugal blowers, specifically at high air flow rates. In addition, there is a significant difference between the characteristic blower curves of centrifugal and PD blowers and this needs to be accounted for in the models.

The energy consumption for blowers, similar to that of pumps, is a function of air flow rate, ambient conditions of the inlet air, efficiencies and discharge pressure. However, the compressibility of air needs to be considered for blowers and this introduces significant differences between the characteristics of aeration systems compared to the characteristics influencing the water and sludge pumps (WEF 2009). The aeration blower process can be described as an adiabatic compression process (Tchobanoglous *et al.* 2004; WEF 2009), which can be defined as a thermodynamic process where no heat is lost or added to the process. Technically this is valid for aeration systems where heat loss to the environment is negligible, e.g. well-insulated systems, where temperature changes in the system are the net result of a change in pressure.

Each blower delivers a certain flow rate (Q_{Air}), decreasing as function of the pressure. This relation is described by the blower characteristic curve (Figure 1), which is as well as the blower efficiency usually provided by the manufacturer. The total pressure or head delivered by the blower shows a monotonic decreasing trend with increasing flow rate, whereas the blower efficiency (Figure 1) shows an optimum with varying flow rate. This optimum is more explicit for centrifugal blowers than for PD blowers. This optimum of the blower efficiency curve is called the best efficiency point (BEP), although the term usually refers to the flow rate at which the best efficiency is reached (Q_{BEP}).

While in operation, a blower experiences a certain pressure, which is both of static and dynamic nature, caused by the system. This varying pressure caused by the system is expressed by the system curve (Figure 1). The most important factors influencing the system curve are (i) the pressure losses in the air line due to friction caused by the piping and in-line equipment, (ii) the diffuser dynamic wet pressure (DWP) and (iii) the water head above the diffuser.

The system curve and the blower curve intersect in one point only, i.e. the duty point or operating point (OP), expressing the only possible flow rate and pressure in that particular system with that particular blower configuration and blower settings (e.g. speed) (Figure 1). The OP also coincides with a certain efficiency and power consumption.

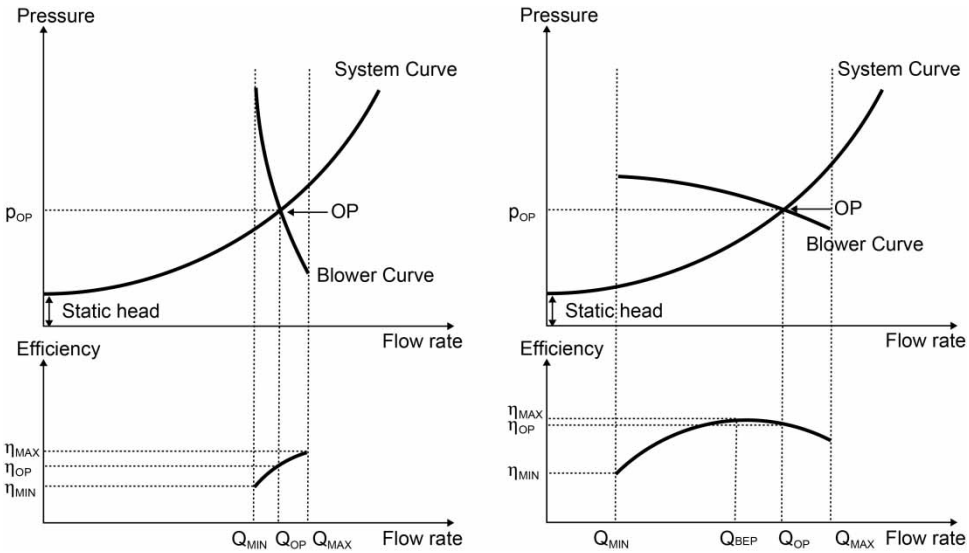

Figure 1 | Schematic representation of the OP or the intersection of the blower curve and the system curve and the corresponding efficiency curve for a PD blower (left) and for a centrifugal blower (right).

For a well-designed system this OP should be as close as possible to the BEP.

The efficiency of centrifugal aeration blowers can have a significant impact on the energy requirement for these units during operation and is dependent on the blower type, design, air conditions and control strategies (Bureau of Energy Efficiency 2006). Blower efficiency is the ratio of the output kinetic energy contained in the airflow stream over the electrical energy input at the wire supply point. The overall energy efficiency of a centrifugal aeration blower (η_t) considers the pneumatic efficiency (η_p), the volumetric efficiency (η_v) (air tightness of the airline), the electrical efficiency (η_e) (including losses incurred from the controller and transformers) and the mechanical efficiency (η_m) (including losses incurred from the motor, bearings and shaft).

Control strategies

Control strategies can be designed to ensure process stability or for the optimization of the overall plant including energy cost. However, changing or controlling the OP, in order to meet operational requirements, can only be established by modifying either the system curve (e.g. by using valves) or the blower curve (e.g. by changing its speed). However, in doing so, the energy requirement of a specific aeration system is changed and should be accounted for in the overall evaluation.

Three control strategies are commonly implemented for aeration blowers: (a) VFD control, (b) variable IGV control and (c) OT (with either an in-line valve or a blow-off valve). The selection of the control strategy is based on the blower type. VFD control can be applied to both centrifugal and PD blowers. Actually, VFD control is the only realistic control strategy to be implemented for PD blowers. With regard to OT both the blow-off valve and the in-line throttling valve are commonly used as a control strategy under operating conditions. A blow-off valve or vane is mostly used (i) at the start-up of large centrifugal blowers in order to reach steady state conditions and (ii) as a security measure to prevent damage due to too high pressures in the aeration system.

A VFD controls the frequency of the alternating current supplied to the blower drive motor, thereby adjusting the blower electric motor rotational speed (Henze 2008). This adjustment in the motor speed results in a shift of the blower curve. This shifted blower curve forces the OP to move along the system curve and results in a new airflow rate versus pressure combination (Figure 2). Additionally, the change in motor rotational speed also alters the efficiency.

Variable IGV control is commonly applied as a control strategy to centrifugal blowers. The design of IGV control is based on rotatable guide vanes fitted at the inlet section, before the impeller, of a centrifugal blower. These guide vanes are commonly straight-blades with low aerodynamic resistance that can adjust within a 90° angle as they are fitted in the inlet air flow path (Xiao *et al.* 2007). In practice, the capacity of most IGV-controlled blowers can only be turned down to about 60% to 80% of the maximum capacity. On adjustment of the guide vanes angle, the OP of the aeration system is shifted due to a change in the blower curve (Boyce 2002).

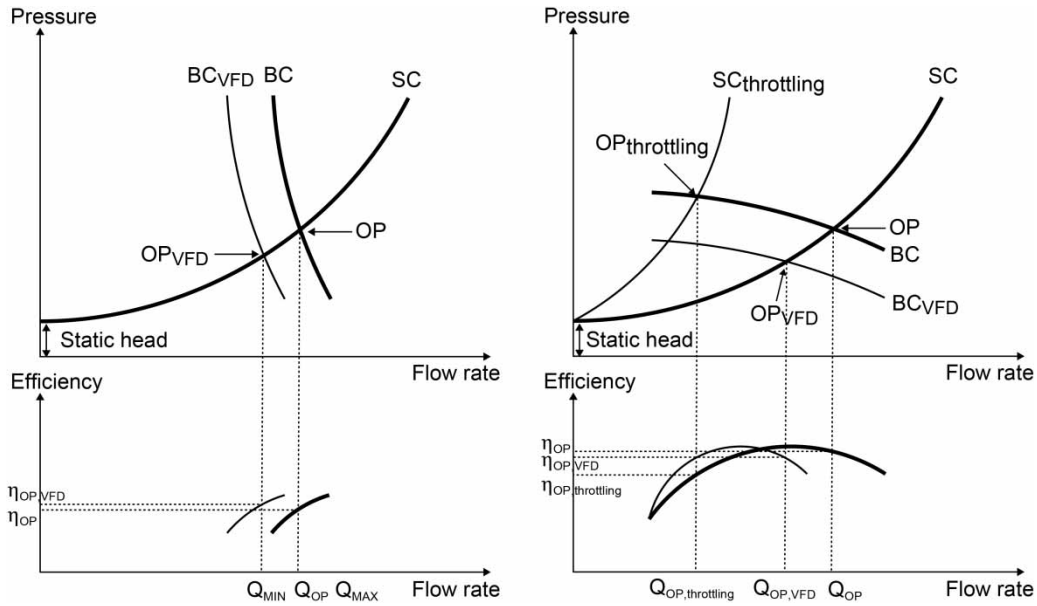

Figure 2 | Schematic representation of different control strategies for PD blowers (left) and centrifugal blowers (right). VFD control shifts both the blower curve (BC towards BC_{VFD}) and the efficiency curve, resulting in a new operating point (OP_{VFD}) and efficiency (η_{VFD}). OT (only applied to centrifugal blowers) shifts the system curve (SC towards $SC_{throttling}$), resulting in a new operating point ($OP_{throttling}$) and efficiency ($\eta_{throttling}$).

Single stage, lower speed centrifugal blowers can be controlled with OT using an in-line valve similar to throttling on centrifugal pumps. The characteristic of the system curve is based on a control valve being fully open (in system design); thus any change in the setting of the control valve will result in an increase in pressure and a change in the system curve, similar to the case of centrifugal pumps. OT is less commonly used as control strategy for aeration systems and will not be addressed in the remainder of the paper.

Mathematical model

In this section, the generic dynamic models that were developed for both uncontrolled and controlled aeration systems are explained. In contrast to textbook knowledge and blower manufacturer data (that are often intended for selecting a blower for a certain application), these models can be used to dynamically calculate the energy consumption of a certain motor-blower combination, thereby accounting for the required flow rate as well as the control actions. The basic assumption is always that the dynamic blower model input is the desired flow rate ($Q_{Air,desired}$), as demanded by the controller, and that the dynamic model outputs are the actual flow rate ($Q_{Air,actual}$) and actual power draw (P_{actual}), given certain blower and system characteristics, which need to be specified by the user. These system characteristics can be parameters that are fixed during the simulation (e.g. the blower curve at full speed, piping layout) or dynamic model inputs that vary in time (e.g. the water level in the aerated tank, air temperature). Note that most equations for variable speed blowers can also be written in terms of the relative blower speed (N) as the independent variable. This allows transforming the model in a way that desired speed is the input signal ($N_{desired}$) rather than $Q_{Air,desired}$. This approach links better to reality, where the WWTP's automatic control system instructs the actuators to run at a certain percentage of their maximum capacity. However, in an integrated water quality modelling context, it is common to use the blower flow rate as the controlled variable.

Key issues to be considered when modelling the energy consumption of aeration systems are: (1) energy requirement for compression, (2) inlet conditions of the air, (3) system characteristic curve, (4) blower characteristic curve, (5) blower efficiency and (6) the type of process control strategy employed.

The mathematical model for the energy requirement for compression

The blower energy consumption, in the case of centrifugal blowers for both fine and coarse bubble diffuser aeration systems, can be estimated using the expression for power requirement P [kW] for adiabatic compression (Tchobanoglous *et al.* 2004). However, considering the significant impact of the

dynamics in the inlet air on the energy requirements, a modified form proposed by WEF (2009) is used (Equation (1)).

$$P(t) = \left(9.816 \cdot 10^{-4}\right) \cdot \left[\frac{Q_{Air,in,N}(t) \cdot p_{in}(t)}{\eta_t(t)} \cdot \left[\left(\frac{p_{out}(t)}{p_{in}(t)}\right)^{n} - 1\right]\right] \quad (1)$$

where $Q_{Air,in,N}$ is the normalized volumetric air flow rate [Nm^3/h] and n is a dimensionless constant for air (0.285) [–]. The number 9.816×10^{-4} lumps constants related to air characteristics (amongst others, the universal gas constant R and the number of moles per volume of air) and those related to the use of $Q_{Air,in,N}$ instead of the air mass flow rate.

In case PD blowers are used, the power consumption can be calculated as in Equation (2) (inspired by WEF (2009)):

$$P(t) = N(t) \cdot Q_0 \cdot (p_{out}(t) - p_{in}(t)) + FPL \quad (2)$$

with N the relative rotational speed [–], Q_0 the blower's theoretical flow rate at full speed, and $p_{out} = p_{in}$ [Nm^3/s] and FPL is the friction power loss at actual operating conditions [kW]. The latter is to be received from the manufacturer, but is typically around 5% of the power consumption at full load (maximum pressure Δp_{max} [kPa]) at that speed N. This means that if FPL would not be available, an acceptable default value could be calculated as in Equations (3) and (4):

$$FPL = FP \cdot (N \cdot Q_0 \cdot \Delta p_{max} + FPL) \quad (3)$$

$$FPL = \frac{FP}{1 - FP} \cdot N \cdot Q_0 \cdot \Delta p_{max} \quad (4)$$

with FP the fraction of the power consumption at full load (0.05 corresponds to 5%).

Data and calculations related to compressible fluids are always expressed in terms of so-called 'standard conditions' to keep everything transparent. The data of the actual input signal (real desired air flow rate Q_{in}) need to be transformed into a normalized desired air flow rate $Q_{Air,in,N}$ (Equation (5)). The definition of standard conditions varies a lot, depending on the application, the country, etc., but 101,325 kPa, 293 K and 50% relative humidity (RH) are common in Europe (International Organization for Standardization 2002).

$$Q_{Air,in,N}(t) = Q_{Air,in}(t) \cdot \left[\left(\frac{101.3}{p_{in}(t) - (RH(t) \cdot PV_a)}\right) \cdot \left(\frac{T_{in}(t)}{273}\right)\right]^{-1} \quad (5)$$

where RH is the relative humidity [–], PV_a is the saturated vapour pressure of water at the actual temperature [kPa], T_{in} is the air temperature at the blower inlet [K], p_{in} is the inlet pressure [kPa], which can be approximated to consider altitude using Equation (6) (The Engineering Toolbox 2005).

$$p_{in} = p_{std}\left(1 - Z \cdot 2.26 \times 10^{-5}\right)^{5.2559} \quad (6)$$

where p_{std} is 101,325 kPa and Z is the altitude above sea level [m].

The mathematical model for the system curve

The flow rate produced by the blower and the corresponding power consumption can be calculated based on the descriptions of the blower curve and the system curve. The latter is calculated based on the pressure developed in the system. The pressure develops due to (i) the pressure losses in the air line caused by friction in the piping and in-line equipment (Δp_{line}), (ii) the diffuser dynamic wet pressure (Δp_{DWP}) and (iii) the water head above the diffuser (Δp_w). The total pressure loss in the system (Δp_{system}) is calculated as the sum of the three pressure losses (Equation (7)).

$$\Delta p_{system}(t) = \Delta p_{line}(t) + \Delta p_{DWP}(t) + \Delta p_w(t) \quad (7)$$

First, pressure or head losses occur within the air pipe lines as a result of pipe line friction losses, bends, fittings and other in-line equipment. Tchobanoglous et al. (2004) quantify the pressure losses based on a modified form of the Darcy–Weisbach equation. Alternatively, WEF (2009) describes the pressure loss in the air line using an empirical formula for air flow in clean steel pipes (Equation (8)).

$$\Delta p_{line}(t) = \left(4 \cdot 10^7 \cdot \frac{Q_{Air,in,N}^{1.85}(t)}{d^5 \cdot p_m(t)} \cdot \frac{T_{in}(t)}{273.15} \cdot \frac{L}{100}\right) + \left(\left(\frac{Q_{Air,in,N}(t)}{4.78 \cdot K_v}\right)^2 \cdot \frac{\rho_{air} \cdot T_{in}(t)}{p_{out}(t)}\right) \quad (8)$$

where T_{in} is the air temperature [K], L is the air line length [m], d is the air line inside diameter [mm], $Q_{Air,in,N}$ is the normalized air flow rate [Nm^3/h], K_v is the valve-specific flow factor [Nm^3/h], ρ_{air} is the relative specific gravity of air [–], p_{out} is the pressure at the blower outlet (= the pipe inlet) [kPa] and p_m is the mean system pressure [kPa]. The value of p_m can be calculated iteratively

according to Equation (9).

$$p_m(t) = p_{out}(t) - \frac{\Delta p_{line}(t)}{2} \tag{9}$$

Friction losses due to fittings are included in this equation via the equivalent pipe length method (Equation (10)).

$$L = L_{pipe} + L_{fittings} = L_{pipe} + \sum_{equiv}^{L} \tag{10}$$

with L_{equiv} the equivalent pipe length [m] of a fitting (Table 1).

Second, the diffuser dynamic wet pressure loss (Δp_{DWP}) is the pressure loss over the fine bubble diffuser membrane, disk or plate during operation under submerged conditions (US EPA Risk Reduction Engineering Laboratory 1989). The variation of DWP with air flow rate is product-specific. Most manufacturers provide this variation in tabulated form (usually two points only). Considering the limited amount of information available a linear approach is adopted (first term in Equation (11)).

The increase of the pressure drop over the diffuser due to membrane fouling is another factor affecting the DWP (Rosso *et al.* 2008). After cleaning, the pressure drop, and consequently the power consumption, returns to approximately its original level.

Dynamic wet pressure loss (Δp_{DWP}) is calculated according to Equation (11), derived from Rosso *et al.* (2008).

$$\Delta p_{DWP}(t) = \left(f_{Diff} \cdot Q_{Air,in,N}(t) + H_0\right) \cdot f_{fouling}(t) \cdot \frac{\rho_w \cdot g}{1000} \tag{11}$$

where $Q_{Air,in,N}$ [Nm^3/h] is the normalized air flow rate, f_{Diff} is the linear pressure loss factor [m $H_2O/(Nm^3/(h{\cdot}m^2))$], H_0 is the cut-off head [m H_2O], ρ_w is the density of the water [kg/m^3] and $f_{fouling}$ is a fouling factor [–]. The latter is a function of time (Equation (12)) and increases linearly from 1 to $f_{fouling,max}$ [–] over a period of $\Delta t_{cleaning}$ [d] (the cleaning interval):

$$f_{fouling}(t) = 1 + \left(f_{fouling,max} - 1\right) \cdot \frac{t - t_{last\ cleaning}}{\Delta t_{cleaning}} \tag{12}$$

with t the current time [d] and $t_{last\ cleaning}$ the last cleaning time [d].

Both f_{Diff} and H_0 can be determined from measuring and plotting the DWP at different airflow rates.

Third, the head loss due to the submersion of the diffusers (Equation (13)) or water head is commonly the most significant contributor to the total system pressure in aeration systems.

$$\Delta p_w(t) = \frac{\rho_w \cdot g \cdot H_w(t)}{1000} \tag{13}$$

where Δp_w is the pressure loss due to the water head [kPa] and H_w is the (variable) water height above the diffuser [m].

Table 1 | Equivalent pipe lengths (as function of the diameter d) (adopted from WEF (2009))

Fitting	Equivalent pipe length [m]
90° elbow	30 d
45° elbow	16 d
T straight through	20 d
T through side	60 d
Transition	20 d
Open butterfly valve	20 d

The mathematical model for the blower curve

The characteristic curve for (single stage) centrifugal blowers (Figure 1, right) can be approximated quantitatively using a power law (Equation (14)), analogous to the approach used to describe the characteristic curve of centrifugal pumps (De Keyser *et al.* 2014).

$$\begin{aligned} p_{blower}(t) &= p_{out}(t) = p_{in}(t) + \Delta p_{system}(t) \\ &= A_{PL} - B_{PL} \cdot Q_{Air,in,N}^{C_{PL}}(t) \end{aligned} \tag{14}$$

where the coefficients A_{PL}, B_{PL} and C_{PL} (Equations (15)–(17)) can be determined as a function of three given (Q_{Air},p) combinations (Figure 3, left).

$$A_{PL} = p_1 \tag{15}$$

$$B_{PL} = (p_1 - p_3) \cdot exp\left(\frac{ln(Q_3) \cdot ln(p_1 - p_3/p_1 - p_2)}{\ln(Q_2/Q_3)}\right) \tag{16}$$

$$C_{PL} = -\left(\frac{ln(p_1 - p_3/p_1 - p_2)}{\ln(Q_2/Q_3)}\right) \tag{17}$$

Note that p_{out}, p_{in}, p_1, p_2 and p_3 are used here as absolute pressures, whereas in most manufacturer data sheets

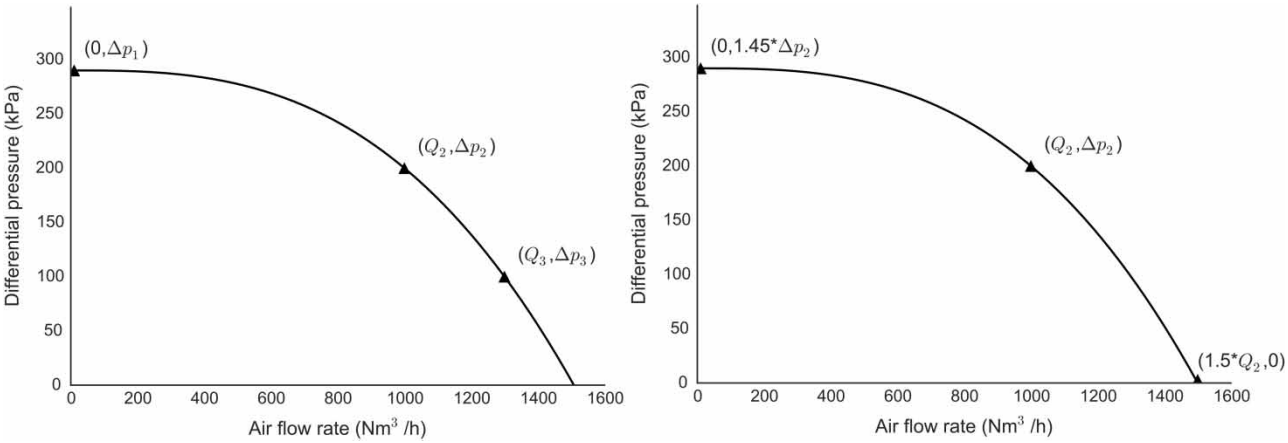

Figure 3 | Centrifugal blower curves constructed following the power law (Equation (14)), based on either three (left) or one (right) flow–pressure combination(s).

only the differential pressure over the blower (Δp_{out}, Δp_1, Δp_2 and Δp_3) is considered.

Following the pragmatic approach for pumps described in Walski *et al.* (2004), this method constructs a blower curve expressing the pressure (p) as a continuous function of the flow rate ($Q_{Air,in,N}$). Point 1 ($0,p_1$) should be the cut-off pressure at zero flow, point 2 (Q_2,p_2) is to be selected in the real operating window of the blower (probably around the BEP), and point 3 (Q_3,p_3) is to be selected at a larger air flow rate. In a situation where no blower curve is available, a default blower curve can be constructed (Figure 3, right) based on the selection of a single desired OP (Q_2,p_2), near a design OP or BEP. The curve is then completed based on the following two assumptions. First, the projected maximum pressure at zero air flow (Δp_1) is 1.45 times Δp_2 and, second, the projected maximum blower flow, at zero pressure loss (i.e. $p_3 = p_{in}$ or $\Delta p_{3=}0$), is 1.5 times Q_2.

For PD blowers the variation of output pressure as a function of flow rate is mainly limited by the blower speed; modifying this speed is generally used to control PD blowers. For this reason, manufacturers generally provide the characteristics of their PD blowers as plots as a function of rotational speed instead of flow rate. However, to be consistent with the approach used for centrifugal pumps, a characteristic curve expressing the pressure as a function of flow rate is used to model the PD blower curves (Figure 4).

For PD blowers, the relation pressure vs. air flow rate is quantified using a quadratic function (Equation (18)). The quadratic function is deemed to be superior to a linear function, which would not be able to describe the (slight) curvature.

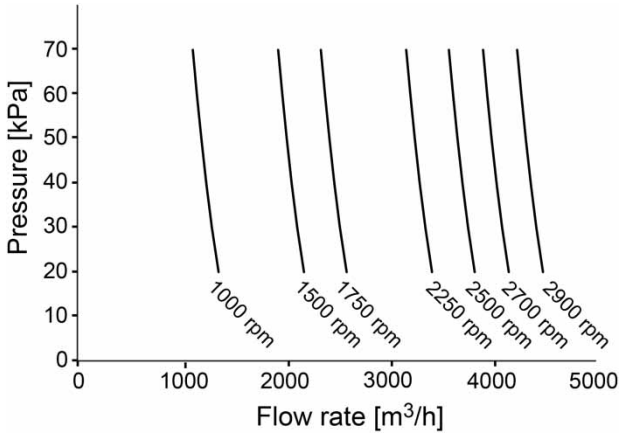

Figure 4 | The change in differential pressure vs. flow rate characteristic of a PD blower (Mapner SEM.40TR) for seven different motor rotational speeds.

$$p_{out}(t) = A_{QL} \cdot Q(t)^2 + B_{QL} \cdot Q(t) + C_{QL} \tag{18}$$

where the coefficients A_{QL}, B_{QL} and C_{QL} (Equations (19)–(21)) can be determined as a function of three given (Q_{Air}, p) combinations (Figure 5, left).

$$A_{QL} = \frac{p_1 \cdot (Q_2 - Q_3) + p_2 \cdot (Q_3 - Q_1) + p_3 \cdot (Q_1 - Q_2)}{Q_1^2 \cdot (Q_2 - Q_3) + Q_2^2 \cdot (Q_3 - Q_1) + Q_3^2 \cdot (Q_1 - Q_2)} \tag{19}$$

$$B_{QL} = \frac{p_1 \cdot (Q_3^2 - Q_2^2) + p_2 \cdot (Q_1^2 - Q_3^2) + p_3 \cdot (Q_2^2 - Q_1^2)}{Q_1^2 \cdot (Q_2 - Q_3) + Q_2^2 \cdot (Q_3 - Q_1) + Q_3^2 \cdot (Q_1 - Q_2)} \tag{20}$$

$$C_{QL} = \frac{p_1 \cdot (Q_2^2 \cdot Q_3 - Q_3^2 \cdot Q_2) + p_2 \cdot (Q_3^2 \cdot Q_1 - Q_1^2 \cdot Q_3) + p_3 \cdot (Q_1^2 \cdot Q_2 - Q_2^2 \cdot Q_1)}{Q_1^2 \cdot (Q_2 - Q_3) + Q_2^2 \cdot (Q_3 - Q_1) + Q_3^2 \cdot (Q_1 - Q_2)} \tag{21}$$

Equation (18) actually describes a parabolic shape, so two solutions are possible: one p_{out} corresponds to two different values for Q_{Air}. Obviously a boundary check is necessary and only the left half of the parabolic function should be used, i.e. for $Q_{Air} \leq Q_{max}$. The latter can be found from the first derivative (Equation (23)) of Equation (22).

$$p_{out} = A_{QL} \cdot Q_{max}^2 + B_{QL} \cdot Q_{max} + C_{QL} \tag{22}$$

$$\frac{dp_{out}}{dQ_{max}} = 2 \cdot A_{QL} \cdot Q_{max} + B_{QL} = 0 \Leftrightarrow Q_{max} = -\frac{B_{QL}}{2 \cdot A_{QL}} \tag{23}$$

In case no characteristic curves of the blower are available, one flow–pressure combination (Q_{design},Δp_{design}) can be used as (Q_1,Δp_1), assuming Δp_{design} to be the maximum pressure to operate against at full speed. The remaining two points are then calculated with Equations (24)–(27).

$$p_2 = p_{in} + 0.5 \cdot \Delta p_1 = p_{in} + 0.5 \cdot (p_1 - p_{in}) = 0.5 \cdot (p_1 + p_{in}) \tag{24}$$

$$p_3 = p_{in} + 0.1 \cdot \Delta p_1 = p_{in} + 0.1 \cdot (p_1 - p_{in}) = 0.1 \cdot p_1 + 0.9 \cdot p_{in} \tag{25}$$

$$Q_2 = 1.1 \cdot Q_1 \tag{26}$$

$$Q_3 = 1.2 \cdot Q_1 \tag{27}$$

The mathematical model for the blower efficiency (η_t)

Determining the actual value for each of the efficiency factors is complex and case specific. In some cases, manufacturers supply overall efficiency factors. The efficiency of centrifugal blowers (Figure 1) typically follows a parabolic trend as a function of the flow rate (Liptak 2005; Bureau of Energy Efficiency 2006). This parabolic trend can be quantified in a similar way as was proposed for centrifugal pumps (Equation (28)).

$$\eta_t(t) = -\left(\frac{\Delta_\eta}{Q_{BEP}^2}\right) \cdot \left(Q_{Air,in,N}(t)\right)^2 + \left(\frac{2 \cdot \Delta_\eta}{Q_{BEP}}\right) \cdot \left(Q_{Air,in,N}(t)\right) + \eta_{min} \tag{28}$$

and

$$\Delta_\eta = \eta_{max} - \eta_{min} \tag{29}$$

with η_{min} the maximum and minimum efficiency [–] respectively, Δ_η the difference between the maximum η_{max} [–] and minimum efficiency, Q_{BEP} the BEP flow rate and $Q_{Air,in,N}$ the normalized flow rate.

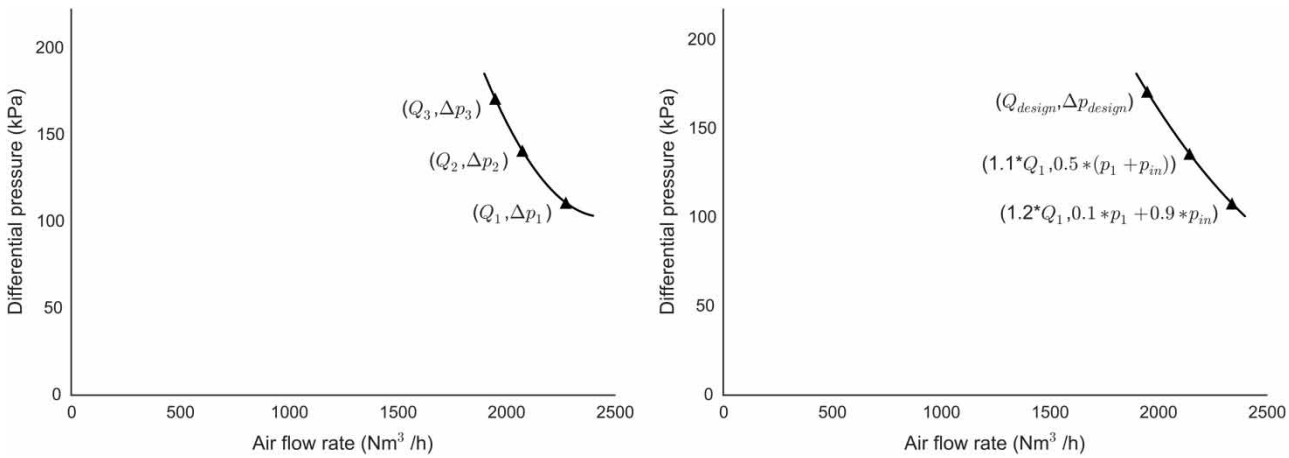

Figure 5 | PD blower curve constructed following the quadratic function (Equation (18)), based on either three (left) or one (right) flow-pressure combination(s).

The efficiency of PD blowers differs from that of centrifugal blowers because they operate in a completely different manner. In the calculation of the power consumption for PD blowers (Equation (2)) the term *FPL*, i.e. the friction power loss at actual operating conditions, was introduced to quantify the efficiency loss induced by the rotary parts causing shear on the inside casing of the blower. This shear depends on the rotational speed and the blower characteristics (Equations (3) and (4)).

The blower efficiency of centrifugal blowers normally transcends that of PD blowers (Henze 2008). For PD blowers, efficiency ranges from 50 to 60% are observed and from 72 to 80% for single stage centrifugal blowers with IGV control.

Mathematical modelling of control for aeration blowers

VFD control. VFD control modifies the rotational speed of the blower and the blower curve shifts accordingly. The relative blower speed N is incorporated in the generic blower curves (Equation (30)), both for centrifugal and PD, by using the affinity laws (Equations (31)–(33)).

$$p_{out}(t) = N(t)^2 \cdot A - B \cdot N(t)^{2-C} \cdot Q_{Air,in,N}^{C}(t) \tag{30}$$

$$\frac{N_1}{N_2} = \frac{Q_1}{Q_2} \tag{31}$$

$$\frac{N_1}{N_2} = \sqrt{\frac{H_1}{H_2}} \tag{32}$$

$$\frac{N_1}{N_2} = \sqrt[3]{\frac{P_1}{P_2}} \tag{33}$$

Since the exponent $2-C$, in Equation (30), is not an integer, an iterative or interpolation method is needed to solve for N. By filling in the desired $Q_{air,in,N}$ and several values for N in Equation (30), the corresponding pressures can be calculated. Next, a linear interpolation yields the N that allows for obtaining the p_{out} that corresponds to $Q_{Air,in,N}$ via the system curve.

At a fixed rotational speed, a centrifugal blower's efficiency shows a parabolic behaviour as a function of the air flow rate (Figure 1, right). However, when a VFD control reduces the speed, this parabolic curve is squeezed towards the origin of the plot (Figure 2, right). This squeezing effect is quantified by introducing the relative blower speed N into Equation (28) (Equation (34)).

$$\eta_t(t) = -\left(\frac{\Delta_\eta}{Q_{BEP}^2}\right) \cdot \left(\frac{Q_{Air,in,N}(t)}{N(t)}\right)^2 + \left(\frac{2 \cdot \Delta_\eta}{Q_{BEP}}\right) \cdot \left(\frac{Q_{Air,in,N}(t)}{N(t)}\right) + \eta_{min} \tag{34}$$

The incorporation of the relative blower speed N [–] in the generic blower curve (Equation (18)) for PD blowers results in Equation (35).

$$p_{out}(t) = A \cdot (Q(t) + Q_0 \cdot (1 - N(t)))^2 + B \cdot (Q(t) + Q_0 \cdot (1 - N(t))) + C \tag{35}$$

with

$$Q_0 = \frac{-B - \sqrt{B^2 - 4A(C - p_{in})}}{2A} \tag{36}$$

where Q_0 [m^3/h] is the flow rate the blower would produce at full speed ($N = 1$) when $p_{out} = p_{in}$.

For PD blowers, the calculation of the efficiency is based on the friction power loss at actual operating conditions (Equations (2)–(4)) and already includes the rotational speed.

IGV control. As variable IGV control is mainly applied as a control strategy to centrifugal blowers, only this application will be dealt with. Determining the efficiency (η_t) for IGV control is different and probably more complex than for VFD control. Unfortunately no quantitative information on IGV-controlled blowers' efficiency was found in literature. Due to the lack of a formula describing the efficiency distribution when using IGV control, a preliminary workaround was developed based on the expected curve for energy requirement.

In the first step the vane setting needs to be determined as an opening fraction. This is achieved by modifying Equation (14), the equation that describes the blower characteristic curve, into Equation (37).

$$f_{IGV}(t) = \frac{Q_{Air,in,N(t)}}{k} \cdot \left(\frac{B}{A - p_{out,IGV}(t)}\right)^{1/C} \tag{37}$$

where f_{IGV} [–] is the guide vane opening fraction (1 = 100% open), k is an experimental scaling factor, $Q_{Air,in,N}$ is the operating flow rate (determined using the system curve), $p_{out,IGV}$ is the outlet pressure (determined using the system curve) and the variables A, B and C can be determined as

described for the derivation of a centrifugal blower curve using Equations (15)–(17).

In the next step the generic efficiency curve presented in Equation (28) needs to be modified to incorporate the guide vane setting into the generic efficiency formula. The resulting Equation (38) can be used to determine the efficiency for IGV control.

$$\eta_t(t) = (-\Delta_\eta \cdot f_{IGV}(t) \cdot \alpha) \cdot \left(\frac{Q_{Air,in,N}(t)}{\beta \cdot f_{IGV}(t) \cdot Q_{BEP}}\right)^2 + \left((2 \cdot \Delta_\eta \cdot f_{IGV}(t) \cdot \alpha) \cdot \left(\frac{Q_{Air,in,N}(t)}{\beta \cdot f_{IGV}(t) \cdot Q_{BEP}}\right)\right) + \eta_{min} \quad (38)$$

with α and β experimental scaling factors.

RESULTS AND DISCUSSION

The model was implemented in the WEST® modelling and simulation software (mikebydhi.com) and applied for the aeration system at the Mekolalde WWTP located in Bergara (Guipúzcoa, Spain). The model is validated in two steps. In the first instance the model is compared to manufacturer data and in the second instance a measurement campaign is conducted.

The Mekolalde WWTP (originally designed to treat wastewater of 40,000 population equivalent) has two primary sedimentation tanks (3 m height and 24 m diameter) followed by three waterlines, of which at the time of the measurement campaign only one was in operation. Each waterline consists of a modified Ludzack–Ettinger process (one denitrification tank of 722 m^3 and three nitrification tanks of 561 m^3 each). Two secondary clarifiers (3 m height and 24 m diameter) separate the sludge from the treated water. The secondary sludge is then further thickened in a dissolved air flotation unit (2 m height and 6 m diameter) and mixed with the primary sludge coming from a thickener (3 m height and 8 m diameter). The sludge is finally further treated in an anaerobic digester (1,600 m^3).

The aeration in the nitrification tanks is provided by five PD blowers of 110 kW each (PD blower Mapner SEM.40TR, Figure 6). Three of them are frequency controlled; the others are on/off controlled (with a soft starter). During the measurement campaign the blowers were manually configured so that one blower provides air to one water line. The air is dispersed through 595 diffusers (SSI™ Fine Bubble Diffusers AFD270 9″ discs) for each of the three lines (1,785 discs in total).

Comparison to manufacturer data

From the manufacturer's technical info sheet (Figure 6), three flow rate–pressure (Q_{Air},p) combinations were derived (at 2,900 rpm, assumed to correspond with $N = 1$) and used as input to the PD blower model: (4,250 Nm^3/h, 70 kPa), (4,375 Nm^3/h, 40 kPa) and (4,575 Nm^3/h, 10 kPa). The water height in the aerated tank was assumed to be constant at 5.7 m above the diffuser surface and the input signal (desired air flow rate during 1 day) varied between 1,615 and 4,500 Nm^3/h with an average of 2,765 Nm^3/h. The aeration system consisted of a 100 m pipe (diameter 0.25 m), 45 m equivalent pipe length for fittings and bends, and a diffuser surface area of 73.23 m^2. The motor efficiency was put at 100% to enable comparison of simulated power consumption with the manufacturer data (the bottom graph in Figure 6 shows the power absorbed at the motor-blower coupling). Other parameters were left at their default values.

Simulations show a nearly constant system pressure, i.e. the impact of the varying flow rate (influencing Δp_{DWP} and Δp_{line}) is small compared to the static head of the liquid Δp_w. Moreover, the simulation results show an excellent match between the predicted air flow rates and the manufacturer data (Table 2). The simulated power consumption, on the other hand, shows a systematic underestimation compared to the manufacturer-supplied power consumption data. The presumed cause is an underestimation of the friction power loss. By adjusting the *FP* in Equation (4) from 5 to 12%, assuming higher friction power losses for this pump type, the predictions improve significantly.

Comparison to real plant data

In the next step the model was confronted with real plant data. The diffuser area was calculated based on the number of diffusers (595) and their active surface area per diffuser (380.9 cm^2). Also the altitude, pipe diameter, pipe length and minor losses equivalent were derived from the system. The flow rates for the definition of the blower curve (Q_1, Q_2 and Q_3) were derived from the manufacturer data.

The parameters to be estimated during the calibration were selected on expert knowledge. For fitting the power consumption the following parameters were estimated using a constrained simplex optimization algorithm (Nelder & Mead 1965): cut-off head, motor efficiency and friction power losses. Moreover, the uncertainty bounds on the estimated parameters are determined using the inverse of the Fisher information matrix (Donckels 2009). After calibration (cut-off head = 160 ± 12 mm H_2O, motor

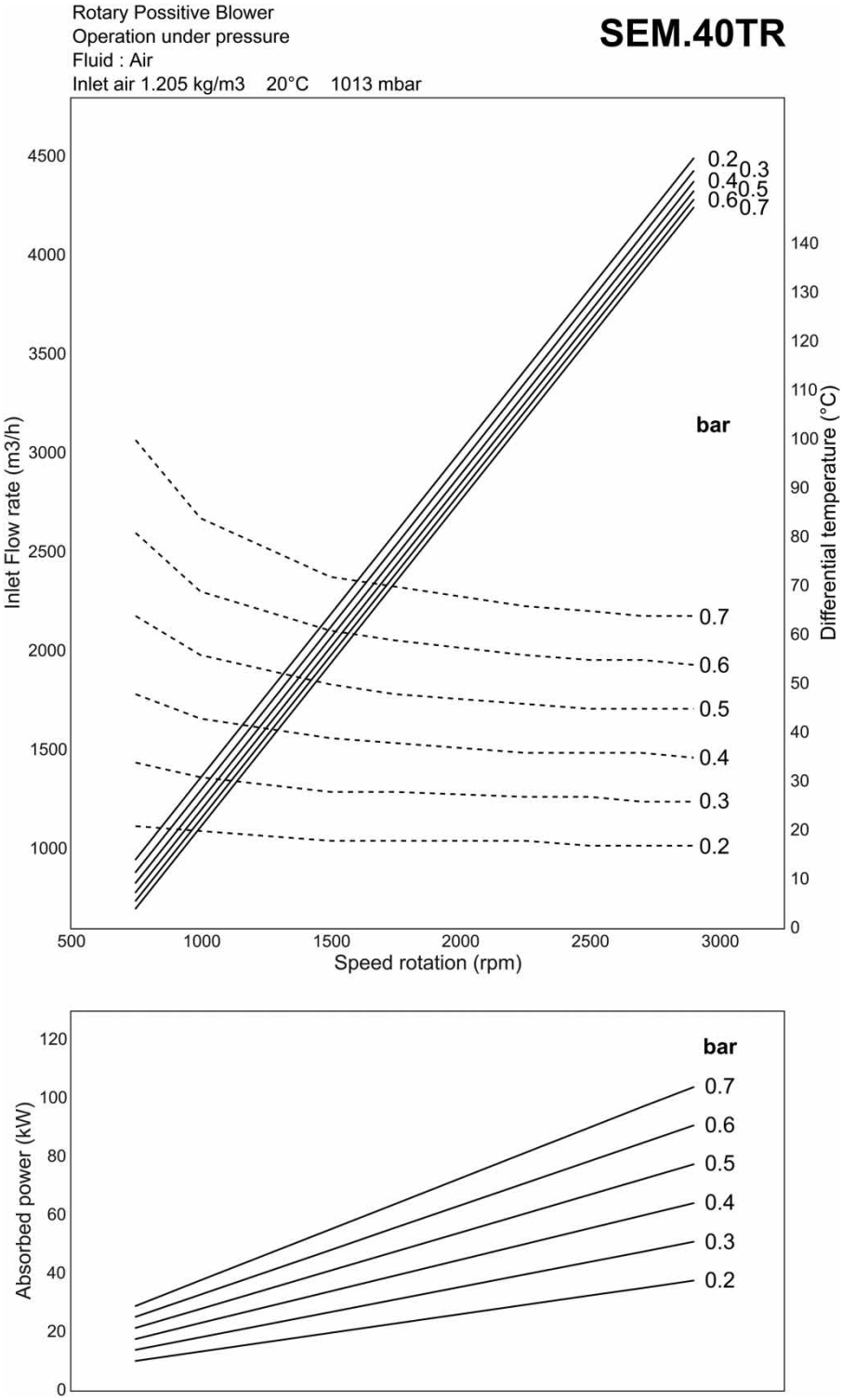

Figure 6 | Redrafted from the technical data sheet for PD blower SEM.40TR (Mapner).

efficiency 0.80 ± 0.03 and friction power losses $= 0.36 \pm 0.02$) the model proved to give an accurate prediction of the real energy consumption by the blowers (Figure 7). The root of the sum of squared errors totalled 1.103 (versus 12.830 with the parameters derived in the comparison with the manufacturer data). A thorough calibration

Table 2 | Comparison between simulation results and manufacturer data for $\Delta p = 60$ kPa

	Air flow rate [Nm³/h]		Power consumption [kW]	
Relative speed *N* [–]	**Simulation**	**Manufacturer**	**Simulation min–max**	**Manufacturer**
1.00 (2,900 rpm)	4,290	4,290	84–91.3	91
0.69 (2,000 rpm)	2,840	2,800	57–62	64
0.51 (1,500 rpm)	1,981	1,980	42–46	48

procedure, which will not be explained here as it falls outside the scope of this paper, results in a slightly better root of the sum of squared errors (1.064 versus 1.103) pointing towards an even better fit (Figure 7). In addition, the uncertainty bounds on the parameter estimates improved drastically ($FP = 9.64 * 10^{-2} \pm 5 * 10^{-5}$, $d = 2.8521 * 10^{-1} \pm 9 * 10^{-5}$ and $\Delta p_3 = 4377.5217 \pm 6 * 10^{-4}$, $\eta_m = 5.502 * 10^{-1} \pm 3 * 10^{-4}$).

Comparison to other models

Comparison is made with constant average power consumption (a fixed ratio power consumption over flow rate) models. The cumulative power consumption shows an exceptional fit to the measured data (Figure 8). On the other hand the model with the constant best fit average

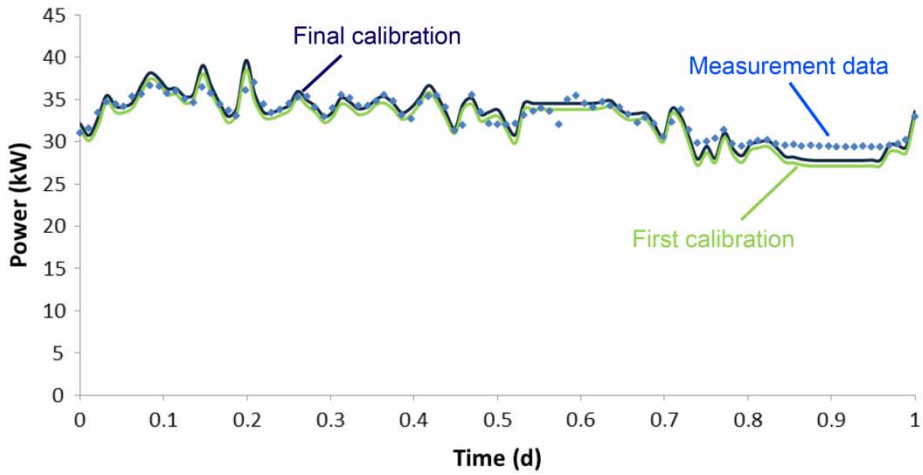

Figure 7 | The final calibrated dynamic model (black line; dark blue in colour version) shows an even better fit, including the trends, to the measurement data (diamonds) then the first calibration attempt (grey line; green line). The full colour version of this figure is available in the online version of this paper: http://dx.doi.org/10.2166/wst.2016.360.

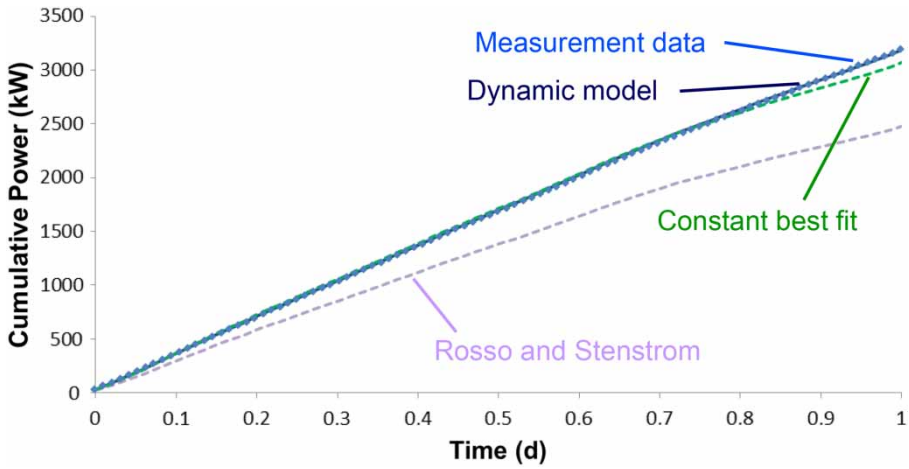

Figure 8 | The exceptional fit of the cumulative power consumption for the dynamic model (black line; dark blue in colour version) to the measurement data (diamonds), outperforms the models with constant average power consumption ratios, although the model with the best fit for the average of the data (dark-grey dashed line, green in colour version) gives also a good fit. The model by Rosso & Stenstrom (2005) (light-grey dashed line; purple in colour version) under-predicts the measured cumulative power consumption. The full colour version of this figure is available in the online version of this paper: http://dx.doi.org/10.2166/wst.2016.360.

power consumption ratio performs excellently as well in regard to the cumulative power consumption. The model by Rosso & Stenstrom (2005) under-predicts the cumulative measured power consumption considerably.

Inspecting the dynamic data (Figure 9), the new detailed dynamic model shows a significantly better fit to the data than the constant average power consumption models. The root of the sum of squared errors for the new detailed dynamic model, the constant average power consumption model based on the parameters determined by Rosso & Stenstrom (2005) and best fit model constant average power consumption model are respectively 1.064, 7.694 and 3.469. Also the sum of squared errors (SSE) reveals the same improvement (112 versus 5,742 and 1,167). The mean of the constant average power consumption model based on the parameters determined by Rosso & Stenstrom (2005) reveals a consistent under-prediction (a mean of 25.5 kW opposed to 32.9 kW for the measured data) explaining the high SSE. This result indicates that the model result and values should not be transferred blindly from one case to another. The best fit constant average power consumption model clearly performs better on the mean value (a mean of 31.7 kW opposed to 32.9 kW for the measured data). But the new detailed dynamic model outperforms both of them (a mean of 32.2 kW opposed to 32.9 kW for the measured data). The main difference, however, is in the variance occurring in the model output. The average consumption models over-predict the variance considerably (a standard deviation of 4.3 kW and 5.3 kW in contrast to 2.3 kW for the measured data) and as such the peak energy demand. On the other hand, the new detailed dynamic model approaches the measured data variance closely (a standard deviation of 2.9 kW opposed to 2.3 kW for the measured data).

In view of a global optimization study for WWTPs, including many different parameters such as effluent quality, energy consumption and greenhouse gas emissions, the newly developed and rigorously calibrated model adds another dimension; i.e. the model restores the balance by adding dynamics in the calculation of the energy consumption, which have a smoothening effect compared with the flow rate data. These dynamic calculations, which are worked out in a high detail as for the influent characteristics and the biokinetic model, allow now for a more accurate estimation of the peak energy demand. This peak energy demand is crucial as it determines the energy price setting.

Furthermore the study demonstrated that care has to be taken when transferring results from another study and a proper evaluation of the background should be performed; i.e. the type of blowers and the system characteristics (height of the water level, type of diffusers, etc.) greatly influence the obtained results.

CONCLUSIONS

A new dynamic model for a more accurate prediction of aeration energy consumption in activated sludge systems, equipped with submerged air distributing diffusers

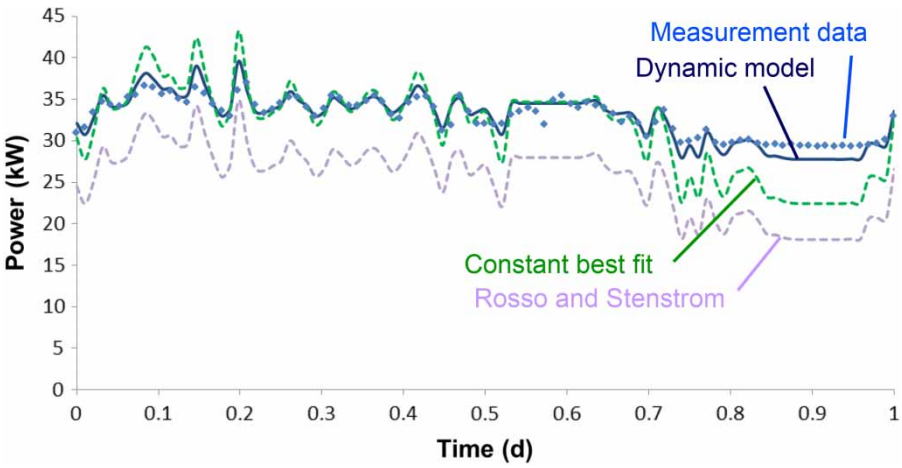

Figure 9 | The dynamic model (black line; dark blue in colour version) describes the measurement data (diamonds) and its trends significantly better than the models with constant average power consumption ratios. Both the model by Rosso & Stenstrom (2005) (light-grey dashed line; purple in colour version) and the model with the best fit for the average of the data (dark-grey dashed line, green in colour version) show larger variations. The full colour version of this figure is available in the online version of this paper: http://dx.doi.org/10.2166/wst.2016.360.

(producing coarse or fine bubbles) connected via piping to blowers, has been developed and demonstrated. The new model proved to give an accurate prediction of the real energy consumption by the blowers and captures the trends better than the constant average power consumption models currently being used. In addition it is demonstrated that transferring model parameters from one installation to another introduces a large risk in incorrectly predicting the power consumption.

The results clearly illustrate, also because the cost of energy depends on peak demand values, that the dynamic model is preferably used in multi-criteria optimization exercises for minimizing the energy consumption. The newly developed model improves the balance in the model complexity between the air supply and demand side. This higher complexity is required, as the knowledge of realistic constraints on the air supply is essential for a correct prediction of the biological reactions. A future extension to improve the model could be the addition of the use of multi-stage blowers instead of single stage blowers.

ACKNOWLEDGEMENTS

The authors would like thank the financial support received from the EU FP7-SME-2008-1 program (project ADD CONTROL 232302) as well all project partners (http://www.addcontrol-fp7.eu/). They would also like to thank the Dommel Waterboard for the data on the energy consumption of their pump.

REFERENCES

Alex, J., To, T. B. & Hartwig, P. 2002 Improved design and optimization of aeration control for WWTPs by dynamic simulation. *Water Science and Technology* **45** (4–5), 365–372.

Amaral, A., Schraa, O., Rieger, L., Gillot, S., Fayolle, Y., Bellandi, G., Amerlinck, Y., Mortier, S. T. F. C., Gori, R., Neves, R. & Nopens, I. 2016 Towards advanced aeration modelling: from blower to bubbles to bulk. In: *Proceedings of the 5th IWA/WEF Wastewater Treatment Modelling seminar, Annecy, France.*

Arnell, M. & Jeppsson, U. 2015 Aeration system modelling – case studies from three full-scale wastewater treatment plants. *9th IWA Symposium on Systems Analysis and Integrated Assessment (Watermatex), Gold Coast, Australia.*

Ast, T., DiBara, M., Hatcher, C., Turgeon, J. & Wizniak, M. O. 2008 Benchmarking wastewater facility energy performance using energy star® portfolio manager. In: *Proceedings of WEFTEC 2008, Chicago, IL, USA*, pp. 7322–7339.

Aymerich, I., Rieger, L., Sobhani, R., Rosso, D. & Corominas, Ll. 2015 The difference between energy consumption and energy cost: modelling energy tariff structures for water resource recovery facilities. *Water Research* **81**, 113–123.

Beltrán, S., Maiza, M., de la Sota, A., Villanueva, J. M., Odriozola, J. & Ayesa, E. 2011 Model-based optimization of aeration systems in WWTPs, *8th IWA Symposium on Systems Analysis and Integrated Assessment (Watermatex), San Sebastián, Spain*, pp. 20–22.

Boyce, M. P. 2002 *Centrifugal Compressors: a Basic Guide*. The Boyce Consultancy Group, Houston, TX, USA, p. 560.

Bureau of Energy Efficiency 2006 *Guide Books 3: Energy Efficiency in Electrical Utilities*. Government of India, Ministry of Power, New Delhi, India.

Copp, J. B. 2002 *The COST Simulation Benchmark – Description and Simulator Manual*. Office for Official Publications of the European Communities, Luxembourg.

De Keyser, W., Amerlinck, Y., Urchegui, G., Harding, T., Maere, T. & Nopens, I. 2014 Detailed dynamic pumping energy models for optimization and control of wastewater applications. *Journal of Water and Climate Change* **5** (3), 299–314.

Devisscher, M., Ciacci, G., Fe, L., Benedetti, L., Bixio, D., Thoeye, C., De Gueldre, G., Marsili-Libelli, S. & Vanrolleghem, P. A. 2006 Estimating costs and benefits of advanced control for wastewater treatment plants – the magic methodology. *Water Science and Technology* **53** (4–5), 215–223.

Donckels, B. 2009 *Optimal Experimental Design to Discriminate Among Rival Dynamic Mathematical Models*, Ghent University, Ghent, Belgium.

Fenu, A., Roels, J., Wambecq, T., De Gussem, K., Thoeye, C., De Gueldre, G. & Van De Steene, B. 2010 Energy audit of a full scale MBR system. *Desalination* **262** (1–3), 121–128.

Flores-Alsina, X., Arnell, M., Amerlinck, Y., Corominas, L., Gernaey, K. V., Guo, L., Lindblom, E., Nopens, I., Porro, J., Shaw, A., Snip, L., Vanrolleghem, P. A. & Jeppsson, U. 2014 Balancing effluent quality, economic cost and greenhouse gas emissions during the evaluation of (plant-wide) control/operational strategies in WWTPs. *Science of The Total Environment* **466–467**, 616–624.

Gernaey, K., Nopens, I., Vrecko, D., Alex, J. & Dudley, J. 2006 An updated proposal for including further detail in the BSM2 PE calculation [internal BSM2 taskgroup document].

Henze, M. 2008 *Biological Wastewater Treatment: Principles, Modeling, and Design*. IWA Publishing, London, UK.

International Organization for Standardization 2002 *Air Intake Filters, ISO 5011:2002*. International Organization for Standardization, Geneva, Switzerland.

Liptak, B. G. 2005 *Instrument Engineers' Handbook. Volume Two: Process Control and Optimization*, 4th edn. Taylor & Francis, London, UK.

Martín de la Vega, P. T., Jaramillo, M. A. & Martínez de Salazar, E. 2013 Upgrading the biological nutrient removal process in decentralized WWTPs based on the intelligent control of alternating aeration cycles. *Chemical Engineering Journal* **232**, 213–220.

Nelder, J. A. & Mead, R. 1965 A simplex method for function minimization. *Computer Journal* **7** (4), 308–313.

Rosso, D. & Stenstrom, M. K. 2005 Comparative economic analysis of the impacts of mean cell retention time and denitrification on aeration systems. *Water Research* **39** (16), 3773–3780.

Rosso, D., Libra, J. A., Wiehe, W. & Stenstrom, M. K. 2008 Membrane properties change in fine-pore aeration diffusers: full-scale variations of transfer efficiency and headloss. *Water Research* **42** (10–11), 2640–2648.

Tchobanoglous, G., Burton, F. L., Metcalf & Eddy, Inc. & Stensel, H. D. 2004 *Wastewater Engineering: Treatment and Reuse*, McGraw-Hill, New York, USA.

The Engineering Toolbox 2005 Air pressure and altitude above sea level. Available from: http://www.engineeringtoolbox.com/air-altitude-pressure-d_462.html.

US EPA Risk Reduction Engineering Laboratory 1989 *Design Manual: Fine Pore Aeration Systems*, US Environmental Protection Agency, Office of Research and Development, Center for Enviromental Research Information, Cincinnati, OH, USA.

Walski, T. M., Barnard, T. E., Harold, E., Merritt, L. B., Walker, N. & Whitman, B. E. 2004 *Wastewater Collection System Modeling and Design*. Haestad Press, Waterbury, CT, USA.

Wambecq, T., Fenu, A., De Gussem, K., Parmentier, G., De Gueldre, G. & Van de Steene, B. 2013 The impact of horizontal water velocity on the energy consumption of a full-scale wastewater treatment plant. *Water and Environment Journal* **27** (2), 247–252.

WEF 2009 *Energy Conservation in Water and Wastewater Facilities – MOP 32*, McGraw-Hill Education, Alexandria, VA, USA.

Xiao, J., Gu, C., Shu, X. & Gao, C. 2007 Performance analysis of a centrifugal compressor with variable inlet guide vanes. *Frontiers of Energy and Power Engineering in China* **1** (4), 473–476.

Zahreddine, P., Dufresne, L., Wheeler, J., Couture, S., Reardon, D. & Henderson, K. 2010 Energy conservation measures for municipal wastewater treatment innovative technologies and practices. In: *Proceedings of the WEFTEC 2010*, New Orleans, LA, USA, pp. 3359–3384.

First received 26 April 2016; accepted in revised form 20 July 2016. Available online 2 August 2016